Cardiac sympathetic-vagal activity initiates a functional brain–body response to emotional arousal

Diego Candia-Rivera[a,b,1] 📷, Vincenzo Catrambone[a,b] 📷, Julian F. Thayer[c,d,e] 📷, Claudio Gentili[f] 📷, and Gaetano Valenza[a,b,1] 📷

A century-long debate on bodily states and emotions persists. While the involvement of bodily activity in emotion physiology is widely recognized, the specificity and causal role of such activity related to brain dynamics has not yet been demonstrated. We hypothesize that the peripheral neural control on cardiovascular activity prompts and sustains brain dynamics during an emotional experience, so these afferent inputs are processed by the brain by triggering a concurrent efferent information transfer to the body. To this end, we investigated the functional brain–heart interplay under emotion elicitation in publicly available data from 62 healthy subjects using a computational model based on synthetic data generation of electroencephalography and electrocardiography signals. Our findings show that sympathovagal activity plays a leading and causal role in initiating the emotional response, in which ascending modulations from vagal activity precede neural dynamics and correlate to the reported level of arousal. The subsequent dynamic interplay observed between the central and autonomic nervous systems sustains the processing of emotional arousal. These findings should be particularly revealing for the psychophysiology and neuroscience of emotions.

emotion | heart-rate variability | EEG | brain–heart interplay | causal theory

"What Is an Emotion?" by William James (1), published more than a century ago, started the scientific debate on the nature of emotions. However, a shared and definitive theory of emotions is not in place yet, and the very definition of emotions and their nature is still a matter of debate. While more "classical" theories point to emotions as "the functional states of the brain that provide causal explanations of certain complex behaviors—like evading a predator or attacking prey" (2), other theories suggest how they are constructions of the world, not reactions to it (3). Namely, emotions are internal states constructed on the basis of previous experiences as predictive schemes to react to external stimuli.

The role of bodily activity in emotions is often questioned. Despite the vast literature showing bodily correlates with emotions, a long-lasting debate about the relationship between bodily states and emotions persists (4). For instance, a feeling is defined as the subjective metarepresentation and labeling of physiological changes (such as an increase in heart rate, the increase of blood pressure, or changes in peristalsis) (5) that are strictly related to the body state on the one hand and to emotions on the other. To this extent, emotions are complex psychological phenomena in which feelings are interpreted and labeled. In a particular psychopathological condition known as alexithymia, individuals experience difficulties in experiencing and understanding emotions to various degrees (6). Indeed, some of these patients can perceive the physical changes connected to a feeling but are unable to label it as emotion, so that emotional experience is described only as its physical counterpart [e.g., described an experience as "I have my heart beating too fast" instead of "I'm fearful" (7)]. From a biological point of view the way in which physical changes become feelings and emotions is based on the interplay between the central and the autonomic nervous systems.

The central nervous system (CNS) communicates with the autonomic nervous system (ANS) through interoceptive neural circuits that contribute to physiological functions beyond homeostatic control, from the emotional experience and the genesis of feelings (8) to decision making (9, 10). The debate about the role of the ANS in emotions can be condensed into two views: specificity or causation (4). The specificity view is related to the James–Lange theory, which states that bodily responses precede emotions' central processing, meaning that bodily states would be a response to the environment, followed by an interpretation carried out by the CNS that would result in the feeling felt. However, causation theories represent an updated view of the James–Lange theory, suggesting that peripheral changes influence the conscious emotional experience; from a biological point of view this may reflect the fact that autonomic nervous signals from the body do influence perceptual activity in the brain

Significance

We investigate the temporal dynamics of brain and cardiac activities in healthy subjects who underwent an emotional elicitation through videos. We demonstrate that, within the first few seconds, emotional stimuli modulate heartbeat activity, which in turn stimulates an emotion intensity (arousal)–specific cortical response. The emotional processing is then sustained by a bidirectional brain–heart interplay, where the perceived arousal level modulates the amplitude of ascending heart-to-brain neural information flow. These findings may constitute fundamental knowledge linking neurophysiology and psychiatric disorders, including the link between depressive symptoms and cardiovascular disorders.

Author affiliations: [a]Bioengineering and Robotics Research Center E. Piaggio, University of Pisa, 56122 Pisa, Italy; [b]Department of Information Engineering, School of Engineering, University of Pisa, 56122 Pisa, Italy; [c]Department of Psychological Science, University of California, Irvine, CA 92697; [d]Department of Biomedical Engineering, University of California, Irvine, CA 92617; [e]Department of Psychology, The Ohio State University, Columbus, OH 43210; and [f]Department of General Psychology, University of Padua, 35131 Padua, Italy

[1]To whom correspondence may be addressed. Email: diego.candia.r@ug.uchile.cl or gaetano.valenza@unipi.it.

(11, 12). In this regard, subjective perception may be influenced or shaped by ascending communication from visceral inputs to the brain (13–15).

Functional models of CNS and ANS interplay have described bidirectional dynamics in emotions (16–18). In particular, the functional brain–heart interplay (BHI) involves brain structures that comprise the central autonomic network (CAN), which has been described as being in charge of autonomic control (19, 20). Moreover, the default mode network (DMN) has been found to be involved in autonomic control (21) and tasks of self-related cognition and interoception (22, 23), suggesting that the DMN participates in both ascending and descending communications with the heart. Finally, the constructed emotion theory suggests how DMN together with other intrinsic networks is crucial in the genesis of emotion and emotional experience (3).

Psychophysiological studies have uncovered several correlates of different autonomic signals in the brain during emotional experiences (24–27). To understand these correlations and the functional interactions between the heart and brain, various signal processing methods have been proposed to investigate functional BHI through noninvasive recordings (28). The study of emotions using these methods comprises the analysis of heartbeat-evoked potentials (29), nonlinear couplings (30), and information transfer modeling (31). However, the causative role of bodily inputs remains unknown (4) and, more specifically, the temporal and causal links between cortical and peripheral neural dynamics in both ascending and descending directions, i.e., from the brain to the body and from the body to the brain, are still to be clarified.

In this study, we take a step forward in answering these scientific questions and investigate whether peripheral neural dynamics play a causal role in the genesis of emotions. We applied a mathematical model of functional BHI based on synthetic data generation (SDG) (32), estimating the directionality of the functional interplay using simultaneous electroencephalography (EEG) and electrocardiography (ECG) recordings gathered from healthy subjects undergoing emotion elicitations with video clips, the publicly available DEAP and MAHNOB datasets (33, 34). ECG series were analyzed to derive heart-rate variability (HRV) series, which result from the concurrent activity of the sympathetic and parasympathetic (vagal) branches of the ANS acting to regulate the heartbeat. We hypothesize that, from a neurobiological point of view, feelings and subsequent emotional experiences arise from the mutual interplay between brain and body, particularly in which the CNS integrates the afferent ANS information outflow, namely from-heart-to-brain interplay, which actually triggers a cascade of cortical neural activations that, in turn, modulate directed neural control onto the heart, namely from brain-to-heart interplay.

Materials and Methods

Dataset Description. This study comprised the analysis of male and female healthy human volunteers from two publicly available datasets undergoing video stimulations with affective content and physiological signals acquisition.

Dataset I. The DEAP dataset for emotion analysis (33) is available at http://www.eecs.qmul.ac.uk/mmv/datasets/deap/. The dataset consisted of 32 subjects who underwent video visualizations. Data were collected at 512 Hz using 32-channel EEG and three-lead ECG. Additional physiological signals were not considered in this study. Data from all subjects were used (age range, 19 to 27 y; median, 27 y; 16 females).

The dataset consisted of 40 video trials from music videos (*SI Appendix,* Fig. S1). Videos had a duration of 60 s and were presented after an initial resting

period of 120 s. Trials have a pad of 5 s at the beginning and 3 s at the end. In this study, the trials were compared to the average initial 120 s rest period.

Dataset II. The MAHNOB–HCI dataset of emotion elicitation (34) is available at https://mahnob-db.eu/hci-tagging/. The dataset consisted of 30 subjects who underwent video visualizations. Data were collected at 256 Hz using 32-channel EEG and three-lead ECG. Additional physiological signals were not considered in this study. A total of 27 subjects participated in the study (age range, 19 to 40 y; median, 26 y; 15 females). Data from individual trials involved a different number of subjects, which ranged between 25 and 27, either because physiological data were not available at the moment (accessed 7 May 2020) or the quality of their ECG was not sufficient to properly identify R-peaks.

The dataset consists of 20 video trials from movies (*SI Appendix,* Fig. S1). Videos had a duration of 35 to 117 s and were presented between neutral videos of ~20-s duration. Trials had a pad of 30 s at the beginning and end. In this study, the trials were compared to the average 30-s rest period before each trial.

Subjective ratings of the emotional experience in the two datasets rely on the circumplex model of affect, which considers a two-dimensional approach to classify emotions: valence related to pleasantness and arousal related to intensity. In this view, emotions can be determined by a linear combination of these two dimensions. We subdivided the trials of the datasets into three groups of emotions, based on group median valence and arousal from the self-assessment scores (*SI Appendix,* Tables S2–S5): pleasant (high valence and high arousal), unpleasant (low valence and high arousal), and low arousal unrelated to valence. For both datasets, the thresholds to define valence and arousal levels were selected independently for the low vs. medium vs. high levels comparison (*SI Appendix,* Table S1A) and the low vs. high levels comparison (*SI Appendix,* Table S1B).

EEG Processing. The aim of the EEG preprocessing was to obtain a clean and artifact-free EEG to consecutively compute the EEG spectrogram. The entire process involves frequency filtering, large artifact removal, eye movements, cardiac-field artifact removal, and interpolation of contaminated electrodes. The process was performed using MATLAB R2018b (MathWorks) and Fieldtrip Toolbox (35). EEG data were bandpass-filtered with a Butterworth filter of order 4, between 0.5 and 45 Hz. Large artifacts were removed using wavelet-enhanced independent component analysis (Wavelet-ICA) (36), which were identified using automated thresholding over the independent component and multiplied by 50 to remove only very large artifacts. EEG data were reconstructed, and ICA was rerun to identify eye movements and cardiac-field artifacts from the EEG data. The process involved one lead from the ECG as an additional input in the ICA to ease the process of finding cardiac artifacts. Once the ICA components with eye movements and cardiac artifacts were visually identified, they were set to zero to reconstruct the EEG series. Individual electrodes were examined under two criteria in the case of noise remnants in the EEG data. Electrodes were marked as contaminated if their area under the curve exceeded three SDs of the mean of all electrodes. The remaining electrodes were compared with their weighted-by-distance-correlation neighbors using the standard Fieldtrip neighbor's definition for a 32-electrode Biosemi system. If a channel resulted in a weighted-by-distance correlation coefficient of less than 0.5, it was considered contaminated. A maximum of three electrodes were discarded per recording by the first criterion, and a maximum of six altogether using the two criteria. After analyzing the EEG electrodes under the second criterion, more than six electrodes were marked as contaminated; only the electrodes with lower correlation coefficients with the neighbors were discarded until only six electrodes were discarded. The contaminated electrodes were replaced by the neighbor's interpolation, as implemented in Fieldtrip. Electrodes were rereferenced offline using a common average (28).

The EEG spectrogram was computed using a short-time Fourier transform with a Hanning taper. The calculations were performed with a sliding time window of 2 s with a 50% overlap, resulting in a spectrogram resolution of 1 s and 0.5 Hz. Successively, time series were integrated within five frequency bands: delta (δ; 0 to 4 Hz), theta (θ; 4 to 8 Hz), alpha (α; 8 to 12 Hz), beta (β; 12 to 30 Hz), and gamma (γ; 30 to 45 Hz).

ECG Processing. The goal of the ECG preprocessing was to obtain R-peak timing occurrences and consecutively compute low- and high-frequency HRV components. The whole process involves frequency filtering, R-peak detection, correction of misdetections, and determination of whether the recording is of optimal quality to be considered in the study. ECG data were bandpass-filtered

using a Butterworth filter of order 4, between 0.5 and 45 Hz. Heartbeats from QRS waves were identified in an automated process based on a template-based method for detecting R-peaks (28). Misdetections were corrected first by visual inspection of detected peaks and the respective interbeat interval histogram and then automatically using a point-process algorithm (37). Recordings presenting segments with unintelligible R-peaks were disqualified from the analysis.

The HRV series were studied in the low-frequency (LF: 0.04 to 0.15 Hz) and high-frequency (HF: 0.15 to 0.4 Hz) ranges to quantify the sympathovagal and parasympathetic activity from the ANS, respectively. Once the heartbeats were detected from the ECG, the HRV series were constructed as the interbeat interval duration time course. Consecutively, the HRV series were evenly resampled at 4 Hz using spline interpolation. The HRV power was computed using a smoothed pseudo-Wigner–Ville distribution (38). The pseudo-Wigner–Ville algorithm consists of a two-dimensional Fourier transform with an ambiguity function kernel to perform two-dimensional filtering. The ambiguity function comprises ellipses whose eccentricities depend on the parameters ν_0 and τ_0, setting the filtering degrees of the time and frequency domains, respectively, and an additional parameter λ was set to control the frequency filter roll-off and kernel tail size (38). The following parameters were considered in this study: $\nu_0 = 0.03$, $\tau_0 = 0.06$, and $\lambda = 0.3$ (32, 38).

Computation of Directional, Functional BHI. Functional BHI was assessed using the SDG model (32), whose software implementation is publicly available at https://github.com/CatramboneVincenzo/Brain-Heart-Interaction-Indexes. The model provides a time course of the estimated coupling coefficients between the different heart and brain components studied separately for both possible modulation directions.

Functional interplay from the brain to the heart. This was quantified through a model able to generate synthetic heartbeat intervals based on an integral pulse frequency modulation model, which is parameterized with Poincaré plot features (39). The synthetic heartbeats were modeled as Dirac functions $\delta(t)$, generating an impulse at the timings of heartbeat occurrences t_k, as presented in Eq. **1**. Heartbeat generation is triggered by the integral of a reference heart rate μ_{HR} and a modulation function $m(t)$, as shown in Eq. **2**, where a new R-peak is generated when the integral function reaches a threshold value of 1.

$$x(t) = \sum_{k=1}^{N} \delta(t - t_k) \qquad [1]$$

$$1 = \int_{t_k}^{t_{k+1}} [\mu_{HR} + m(t)]\, dt \qquad [2]$$

The modulation function $m(t)$ is represented as a summation of two oscillators on behalf of the sympathetic and parasympathetic autonomic outflows, as presented in Eq. **3**. The oscillators are centered at the frequencies ω_s and ω_p, with amplitudes defined by C_S and C_P indicating time-varying coupling constants, representing the sympathetic and parasympathetic activities, respectively. The coupling constants are defined in Eqs. **4** and **5**, where the parameters L and W are the length and width of the Poincaré plot (39) and $\gamma = \sin(\omega_p/2\mu_{HR}) - \sin(\omega_s/2\mu_{HR})$.

$$m(t) = C_S(t) \cdot \sin(\omega_s t) + C_P(t) \cdot \sin(\omega_p t) \qquad [3]$$

$$\begin{bmatrix} C_S \\ C_P \end{bmatrix} = \frac{1}{\gamma} \begin{bmatrix} \dfrac{\sin(\omega_p / 2\mu_{HR})\, \omega_s\, \mu_{HR}}{4\sin(\omega_s / 2\mu_{HR})} & \dfrac{-\sqrt{2}\, \omega_s\, \mu_{HR}}{8\sin(\omega_s / 2\mu_{HR})} \\ \dfrac{-\sin(\omega_s / 2\mu_{HR})\, \omega_p\, \mu_{HR}}{4\sin(\omega_p / 2\mu_{HR})} & \dfrac{\sqrt{2}\, \omega_p\, \mu_{HR}}{8\sin(\omega_p / 2\mu_{HR})} \end{bmatrix} \begin{bmatrix} L \\ W \end{bmatrix} \qquad [4]$$

The model considers the interaction from the CNS as the ratio between the coupling constants (i.e., C_S and C_P) and the EEG power in the previous time window $\mathrm{Power}_f(t-1)$ at a defined frequency band f (i.e., δ, θ, α, β, and γ). Therefore, the BHI coefficients $\mathrm{SDG}_{\mathrm{brain}_f \to LF}$ and $\mathrm{SDG}_{\mathrm{brain}_f \to -HF}$ are defined by Eqs. **5** and **6**, respectively.

$$\mathrm{SDG}_{\mathrm{brain} \to LF}(t) = C_S(t)\, /\, \mathrm{Power}_f(t-1) \qquad [5]$$

$$\mathrm{SDG}_{\mathrm{brain} \to HF}(t) = C_P(t)\, /\, \mathrm{Power}_f(t-1) \qquad [6]$$

Functional interplay from the heart to the brain. The functional interplay from the heart to the brain is quantified through a model based on the generation of synthetic EEG series using an adaptive Markov process (40), as shown in

Eq. **7**. The model estimates the modulations to the brain expressed by the coefficient Ψ_f using least squares in an exogenous autoregressive process, as shown in Eq. **8**, where f is the main frequency in a defined frequency band, θ_f is the phase, κ_f is a constant, and ε_f is a Gaussian white noise term.

$$EEG(t) = \sum_{f=f_1}^{f_n} \mathrm{Power}_f(t) \cdot \sin(\omega_s t + \theta_f) \qquad [7]$$

$$\mathrm{Power}_f(t) = \kappa_f \cdot \mathrm{Power}_f(t-1) + \Psi_f(t-1) + \varepsilon_f \qquad [8]$$

Therefore, the Markovian neural activity generation within a specific EEG channel and frequency band uses its previous neural activity and heartbeat dynamics as inputs for EEG data generation. The coupling coefficients $\mathrm{SDG}_{\mathrm{heart} \to \mathrm{brain}}$ can be derived from the contribution of heartbeat dynamics HRV_X (with X as LF, HF, or their combination) and the exogenous term of the autoregressive model:

$$\mathrm{SDG}_{X \to \mathrm{brain}}(t) = \Psi_f(t)\, /\, HRV_X(t). \qquad [9]$$

For this study, the model computed the coefficients using a 15-s-long time window with a 1-s step to estimate the coefficients. The central frequencies used were $\omega_s = 2\pi \cdot 0.1$ rad/s and $\omega_p = 2\pi \cdot 0.25$ rad/s, in which 0.1 Hz and 0.25 Hz correspond to LF and HF band central frequencies, respectively.

As a noise-control measure, we performed a simulation study aimed to assess the aforementioned SDG model sensitivity to random input variability. In particular, we randomly selected real physiological signals comprising series of EEG power in the θ band, series of LF and HF powers from heartbeat dynamics, and RR series and randomly added variability through white random noise ε at increasing variance σ. Variances were proportional to the original variances of the series, and this proportionality coefficients ranged in $\phi \in [0.2\ 0.5\ 1\ 2\ 5\ 10]$. The new series, represented as PSD_θ^1, PSD_{HF}^1, PSD_{LF}^1, RR^1 respectively, are mathematically expressed as

$$\mathrm{PSD}_\theta^1 = \mathrm{PSD}_\theta^0 + \phi_i \sigma_{\mathrm{PSD}_\theta^0} \varepsilon \qquad [10]$$

$$\mathrm{PSD}_{HF}^1 = \mathrm{PSD}_{HF}^0 + \phi_i \sigma_{\mathrm{PSD}_{HF}^0} \varepsilon \qquad [11]$$

$$RR^1 = RR^0 + \frac{\phi_i \sigma_{RR^0}}{10} \varepsilon. \qquad [12]$$

Results of the simulation study are shown in *SI Appendix*, Figs. S10–S13 and indicate that the brain–heart coupling decreases in all functional directions as the variability of additive noise increases.

EEG Correlates of Attention. In order to disentangle the role of attention processes from the emotional experience in the investigation of functional BHI coupling, we estimated two EEG-based correlates of attention. One attention marker is based on central-right alpha power (41) that has been shown to correlate with the subjective experience of attention as estimated through self-ratings and pupil diameter (41). The second attention marker is based on frontal beta power (42) and has been validated in a spatial attention task (42).

Statistical Analysis. The samples were described groupwise using the median, and the related dispersion measures were expressed as median absolute deviation. Statistical analyses included the Spearman correlation coefficient, Friedman tests, and cluster-based permutation test. Spearman correlation was performed groupwise over individual electrodes to determine the relationships between the group-median brain–heart coupling coefficients and associated valence or arousal dimensions. Spearman P values were derived using a Student's t distribution approximation. Friedman tests were performed to assess statistical changes in the BHI coupling coefficients per EEG electrodes, on different time windows, and considering different types of trials (pleasant, unpleasant, or neutral). The significance level of the P values was corrected per the Bonferroni rule, considering the multiple comparisons performed for the 32 EEG electrodes, with an uncorrected statistical significance set to $\alpha = 0.05$.

Cluster-based permutation tests (43) were performed over the coupling coefficients between the averaged rest period and the trial of emotion elicitation in their total duration. The comparisons were performed for LF→brain, HF→brain, brain→LF, and brain→HF indices, where the brain part comprises 32 EEG electrodes, the time course, and the five frequency bands studied. The nonparametric cluster-based permutation tests include a preliminary mask definition, identification of candidate clusters, and computation of cluster statistics with Monte Carlo P value correction. The preliminary mask was computed by

performing a paired Wilcoxon test for individual samples defined in space, time, and frequency. If a sample obtained a P value lower than $\alpha = 0.01$, the sample was considered part of the preliminary mask. Candidate clusters were formed first on individual timestamps and separately for each frequency band. The identification of neighbor electrodes was based on the default electrodes' neighborhood definition for a 32-electrode Biosemi system in the Fieldtrip Toolbox. A minimum cluster size of the three electrodes was imposed. Adjacent candidate clusters on time were wrapped if they had at least one common channel. Adjacent candidate clusters on frequency were wrapped if they had at least one pair (channel, timestamp) in common. The overall minimum duration of the cluster was set at 2 s. Cluster statistics were computed from 10,000 random partitions. The data points defined by the cluster's mask in the space, time, and frequency dimensions were averaged. The samples of the two experimental conditions (rest and emotion elicitation) were placed in a single set. Therefore, samples from the two conditions were randomly selected, and a nonparametric Wilcoxon test was performed over the random partition. The proportion of random partitions that resulted in a lower P value than the observed one was considered as the Monte Carlo P value. The cluster's Monte Carlo P value was considered to be significant at $\alpha = 0.01$. The cluster statistic considered is the Wilcoxon's Z-value obtained from the test on the averaged data points defined by the mask, and the resulting P value is reported as well. If more than 1, the cluster with the highest absolute Z-value was considered.

Results

Resting State vs. Emotion Elicitation. We computed the BHI coupling coefficients at individual EEG electrodes for all trials and resting sessions. The output of the model was the time course of the coupling for all combinations of brain oscillations (delta, theta, alpha, beta, and gamma) and HRV LF and HF components. Fig. 1 shows the number of trials in the two datasets in which the heart-to-brain or brain-to-heart interplay coefficients presented a significant change with respect to the resting state, in accordance with a nonparametric cluster-based permutation analysis; *SI Appendix*, Figs. S3 and S4 show the scalp distribution of such significant BHI coupling coefficients. Thirty-nine out of the 40 trials in the DEAP dataset and 17 out of 20 trials in the MAHNOB dataset presented a significant cluster in either the ascending or descending directions (*SI Appendix*, Tables S6–S11). HF-to-brain and brain-to-HF coupling coefficients were more sensitive markers of emotion elicitation than LF-to-brain and brain-to-LF. Ascending sympathovagal activity (LF power) tends to sustain EEG oscillations in the theta, alpha, and beta bands, while ascending vagal activity (HF power) sustains EEG oscillations at all frequencies, with a reduced number of trials associated with the gamma band. Such ascending HF-to-brain interplay presented overall higher amplitude over the midline frontal and occipitoparietal electrodes. In the brain-to-heart interplay, the LF band is considerably less coupled to the brain than the HF band, which is modulated by EEG oscillations at all frequency bands. The descending brain-to-heart interplay presented coupling coefficients with a lower amplitude during emotion elicitation, especially over the central regions, at all EEG frequency bands.

Since significant changes in BHI coupling for emotion elicitations are associated mainly with cardiac vagal activity, for the sake of conciseness the results presented below refer to cardiac HF power. Further experimental results on cardiac LF power are reported in *SI Appendix*.

Correlation Analysis between Emotion Self-Assessment Scores and Directional BHI Coefficients. We explored group-wise correlations between the BHI coupling coefficients and perceived (self-reported) arousal and valence. Especially in the DEAP dataset, we found that ascending vagal activity (HF power) modulation to EEG oscillations in the delta, theta, and gamma bands correlate with the reported arousal scores (Fig. 2*A*, arousal). Alternately, nonsignificant and lower Spearman correlation coefficients were associated with valence scores (Fig. 2*A*, valence). HF-to-delta interplay was significantly correlated in the occipitoparietal, left-central, and frontal electrodes. HF-to-theta was correlated in the occipitoparietal and frontal electrodes, and HF-to-gamma over both temporal regions. On the other hand, single-system estimates related HF power, and EEG power in the delta, theta, and gamma bands did not significantly correlate with perceived arousal (*SI Appendix*, Fig. S5). The BHI coupling coefficients and arousal scores were compared to two different neural correlates of attention: marker 1 based on central alpha power (41) and marker 2 based on frontal beta power (42). Fig. 2*C* shows that none of the markers correlated with BHI coupling coefficients, and only marker 2 slightly anticorrelated with the arousal scores (though in a nonstatistically significant fashion provided a correction for multiple comparisons). As shown in Fig. 2*D*, none of the two attention markers may discern emotional valence groups as SDG coefficients do (Wilcoxon paired test on: unpleasant vs. neutral, $P = 0.0346$, $Z = 2.1130$; pleasant vs. unpleasant, $P = 0.0004$, $Z = 3.4967$; pleasant vs. neutral, $P < 0.0001$, $Z = 4.0951$).

The aforementioned results suggest that subjective emotional arousal modulates ascending functional BHI coupling whose changes are not related to attention.

Directional BHI at Different Arousal and Valence Levels. We investigated statistical differences between low, medium, and high arousal and valence for the directional BHI coupling coefficients. The low, medium, and high valence/arousal groups were selected based on the group-median values from the self-assessment scores. The trials between the low-medium and medium-high values were not considered for further analyses to avoid overlap between the levels of valence/arousal (*SI Appendix*, Table S1A). In Fig. 3 the results of the Friedman test for HF-to-brain and brain-to-HF are shown for the three levels of arousal. The results indicate that in both datasets there is a relatively higher relation to changes in arousal for ascending BHI with respect to descending coupling coefficients, since this variability with respect to arousal in the DEAP dataset is stronger and significant after multiple comparison corrections.

In Fig. 4 the results of the Friedman tests for HF-to-brain and brain-to-HF couplings are shown for the three levels of valence.
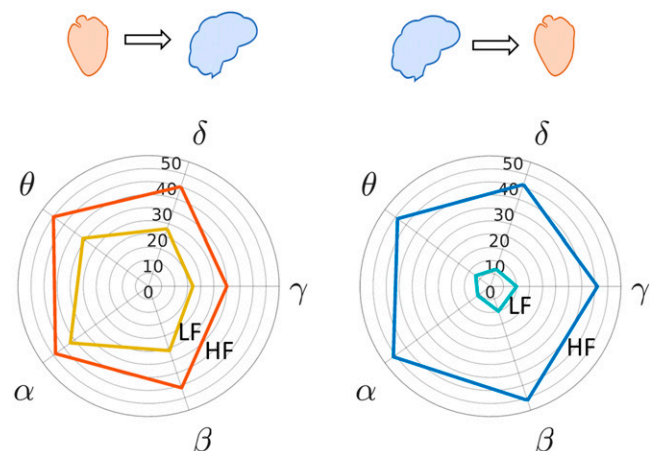

Fig. 1. Polar histograms showing the number of trials in the two datasets (60 trials) in which the respective heart-to-brain and brain-to-heart components showed a significant change in the cluster-based permutation analysis with respect to the resting state. The radial axis indicates the trials' count, and the angle axis indicates the EEG frequency band. (*Left*) Heart-to-brain interplay and (*Right*) brain-to-heart interplay (see *SI Appendix*, Fig. S2 for polar histograms of pleasant, unpleasant, and neutral trials).
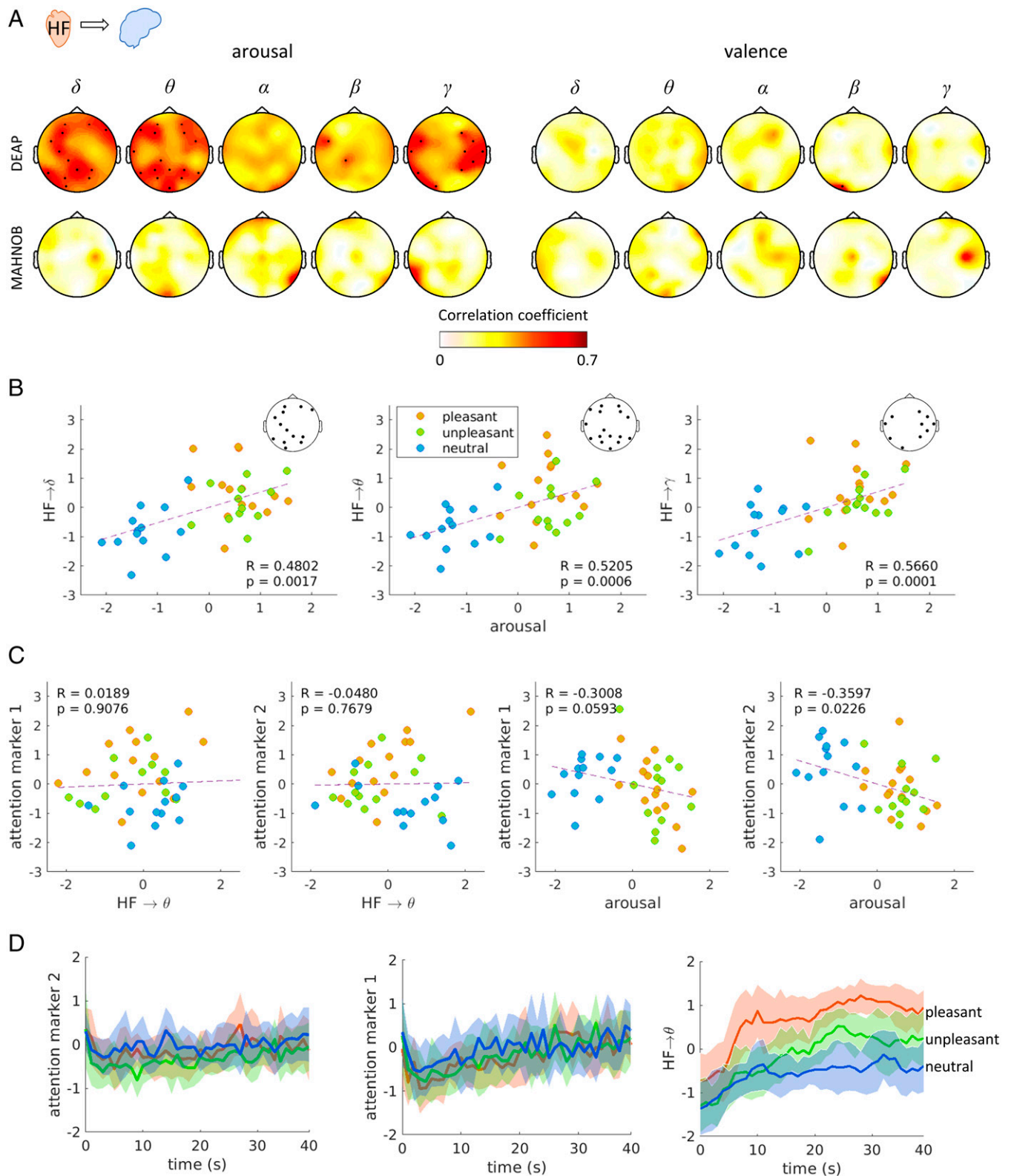
Fig. 2. Correlation analysis between ascending BHI coupling coefficients and self-reported arousal and neural correlates of attention. Each point corresponds to the group-median calculated per trial. Individual values were previously normalized (max-min norm) within all trials for each subject. (*A*) Correlation between trials' median arousal and HF-to-brain median coefficients. Colormaps indicate the magnitude of correlation coefficients, and thick electrodes indicate significant correlation corrected for multiple comparisons among electrodes ($P < 0.05/32$). (*B*) Scatter plot of perceived arousal and HF→δ, HF→θ, and HF→γ coupling coefficients in the electrodes where a significant correlation was found. (*C*) Scatter plot of attention markers and perceived arousal and HF→θ coupling coefficient. Attention marker 1 is computed from EEG alpha power in channel C4 and CP2 (41). Attention marker 2 is computed from EEG beta power in frontal electrodes (42). (*D*) Group-median ± median absolute deviation (MAD) time course from the trial video onset of the attention marker 1 (*Left*), attention marker 2 (*Middle*), and HF→θ interplay (*Right*), separated for emotional valence. The HF→θ time course corresponds to the average among all electrodes with a significant correlation with arousal, as shown in *A*.
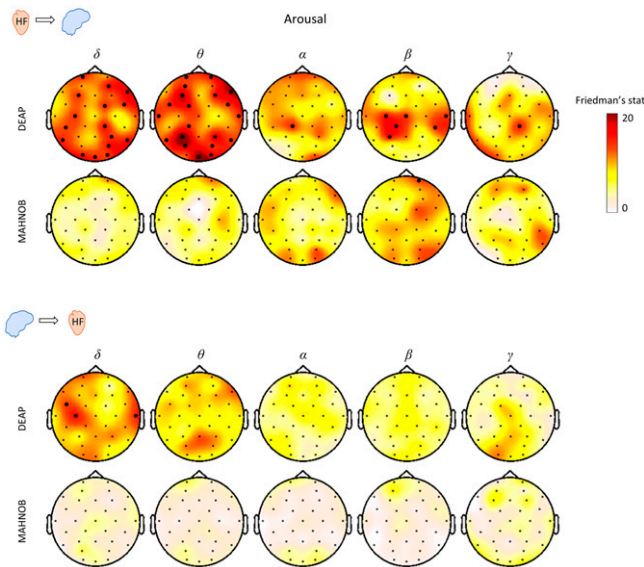
Fig. 3. Scalp distribution of the Friedman test statistics for the HF-to-brain and brain-to-HF comparison between three levels of arousal. Trials for each group of arousals were averaged separately for the two datasets. Colormaps indicate the amplitudes of the respective Friedman statistic and thick electrodes indicate significance ($P < 0.05/32$).

The results indicate that there is no strong relation to the variability of valence as shown for arousal in Fig. 3. In fact, we can observe only a small significant cluster in HF-to-theta in the DEAP dataset and another in HF-to-beta in the MAHNOB dataset.

Qualitatively, the aforementioned results indicate that changes in the reported arousal are associated with a stronger modulation of BHI, as expressed in the SDG coupling coefficients, rather than changes in the reported valence, especially in the functional modulation from the heart to the brain.

To further investigate the BHI modulation occurring along the valence and arousal dimensions, we performed a statistical analysis on selected trials to compare the levels of arousal at an equal valence, and to compare levels of valence at equal arousal. To do so, we performed a cluster permutation analysis in the spatial dimension. In the MAHNOB dataset the coupling coefficients do not discriminate between low and high arousal or valence. In the DEAP dataset, the results indicate that the ascending HF-to-brain coupling repeatedly showed differences between levels of arousal, for either a low or high valence, whereas the levels of valence do not show significant differences as shown in Fig. 5.

Temporal Dynamics of the Directional Brain–Heart Coefficients under Emotion Elicitation. We further investigated the overall variability of the BHI coupling coefficients over time. To this end, we performed groupwise Friedman tests to compare the resting state and emotion elicitation at different latencies, among all-trials-median. These results indicate that significant changes occurred among the conditions especially in the ascending direction in the delta, theta, alpha, beta, and gamma bands, with a strong agreement in HF-to-theta in midline parieto-occipital scalp region in the DEAP and MAHNOB datasets. The descending interplay presented a major variability on time over the HF-to-theta and HF-to-alpha on central scalp regions (*SI Appendix*, Fig. S6).

In Fig. 6 the group-medians time course of all trials average are aligned in the trial offset and separated for both datasets. The displayed BHI components correspond to the SDG coefficients presenting a strong variability on time in ascending and descending interplay, as measured with Friedman test (*SI Appendix*, Fig. S6). HF-to-theta interplay indicates an overall

increase in the SDG coefficient amplitudes during the video visualization, whereas theta-to-HF in the opposite direction presents a decay toward the video end (to see other examples, see *SI Appendix*, Fig. S15).

The BHI temporal dynamics show that the physiological processes involved in emotion elicitation cause changes in both heart-to-brain and brain-to-heart interplay, with an anticorrelated behavior during the video visualization period. Major differences were found in the interval 20 to 30 s with respect to the trial onset in both datasets, indicating that after 20 s there is an increase in the variability of the SDG coefficients (*SI Appendix*, Fig. S7).

Fig. 7 shows an overall representation of the DEAP dataset, in which the trials' counts (separated as unpleasant, pleasant, and neutral) presented a significant change in relation to the resting state at different latencies in the cluster-based permutation analysis. It should be noted that it was not possible to draw an analogous figure for the MAHNOB dataset because different videos had different durations. It can be observed that the 20- to 30-s latency presents major differences between unpleasant, pleasant, and neutral trials, as reported above. We can also observe that the pleasant and unpleasant emotions present more trials with a significant change overall when compared to the neutral trials. Importantly, heart-to-brain interplay tends to occur earlier compared to the brain-to-heart interplay. However, brain-to-heart interplay tends to last longer toward the end of the video visualization. Although cardiac vagal activity sustains the BHI coupling throughout the elicitation, LF power as modulated by overlapped sympathetic-vagal activity is involved especially in the ascending pathway, as observed mainly in pleasant and unpleasant trials in later stages of video clip visualizations.

Finally, here we show two examples to better illustrate the brain-heart dynamics contrasting high-arousing, pleasant and unpleasant emotional elicitation (to visualize a single subject example see *SI Appendix*, Fig. S8). Fig. 6 shows the evolution of SDG coefficients at different latencies (to visualize an exemplary case for the SDG time courses for one subject see *SI Appendix*). In *SI Appendix*, Fig. S16A, we observed an example taken from the DEAP dataset corresponding to an extract of the music video "The One I Once Was," by the Norwegian
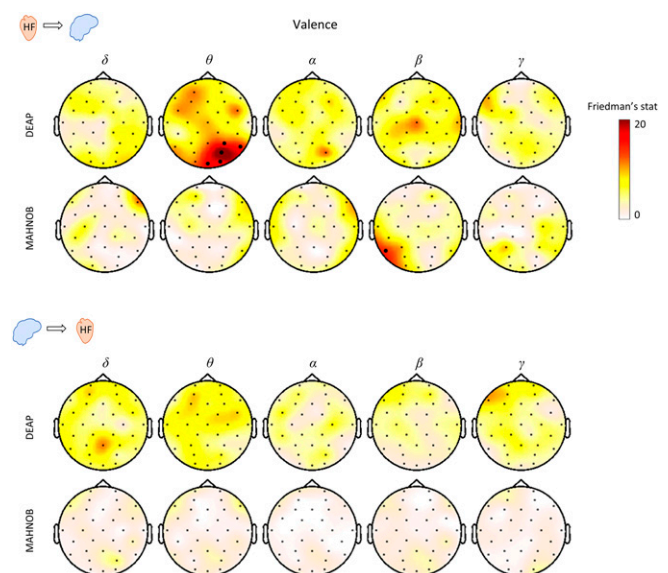

Fig. 4. Scalp distribution of the Friedman test statistics for the HF-to-brain and brain-to-HF comparison between three levels of valence. Trials for each group of arousals were averaged separately for the two datasets. Colormaps indicate the amplitudes of the respective Friedman statistic and thick electrodes indicate significance ($P < 0.05/32$).
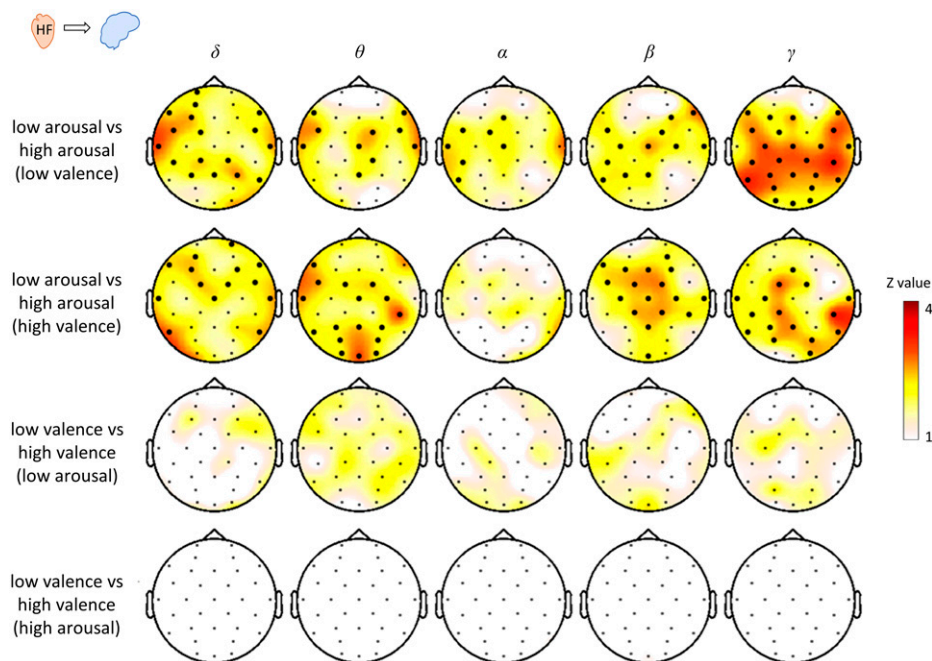
Fig. 5. Comparison of HF-to-brain interplay between emotion groups: pleasant, unpleasant, and neutral from the DEAP dataset. The comparison corresponds to the average in time and average among the selected trials with equal arousal or valence (*SI Appendix*, Table S1B). The comparisons were performed per channel and frequency band separately. The statistical comparison corresponds to one-dimensional cluster permutation analysis with alpha level for the preliminary mask set at $P < 0.05$. Thick electrodes indicate clustered effects at $P < 0.05$ after 10,000 random permutations. Scalp topographies indicate the Z-value obtained from the pairwise Wilcoxon test.

band Mortemia. We placed this music video in the group of unpleasant trials based on the valence and arousal self-assessment performed by the subjects in this study. The video starts with a close-up of an executioner where activation is immediately observed on the parietal scalp region in the HF-to-brain interplay, followed by an overall scalp change from the brain-to-HF interplay. The video continues with the execution of a man, in which the whole process causes an overall activation of the scalp in the HF-to-brain interplay, still focused on parietal electrodes. Around the 30th second, the man is executed, and a higher coupling appears on frontal electrodes in the HF-to-brain interplay, an overall scalp activation of lower amplitude appears in the LF-to-brain interplay, and the brain-to-HF interplay is maintained with a stronger coupling on central electrodes. The video is followed by a deceased man accompanied by two

nuns and a cemetery scene, where a decrease in the coupling coefficients is observed with the HF-to-brain, which lasts longer.

In *SI Appendix*, Fig. S16B, we observed an example taken from the MAHNOB dataset corresponding to an extract of the 2003 film *Love Actually*, a romantic comedy by Richard Curtis. We placed this trial in the group of pleasant trials based on valence and arousal self-assessments performed by the subjects of this study. The video starts with a priest finishing a wedding ceremony; when the applause and instrumental wedding music begin, the man kisses the bride, and activation on the parietal region in the HF-to-brain interplay is observed. LF-to-brain interplay appears in the left frontal scalp region when a short dialogue occurs, followed by the start of choral music and progressively appearing musicians from random positions inside the church, playing a cover version of "All You Need Is Love" by The Beatles. During the music, strong
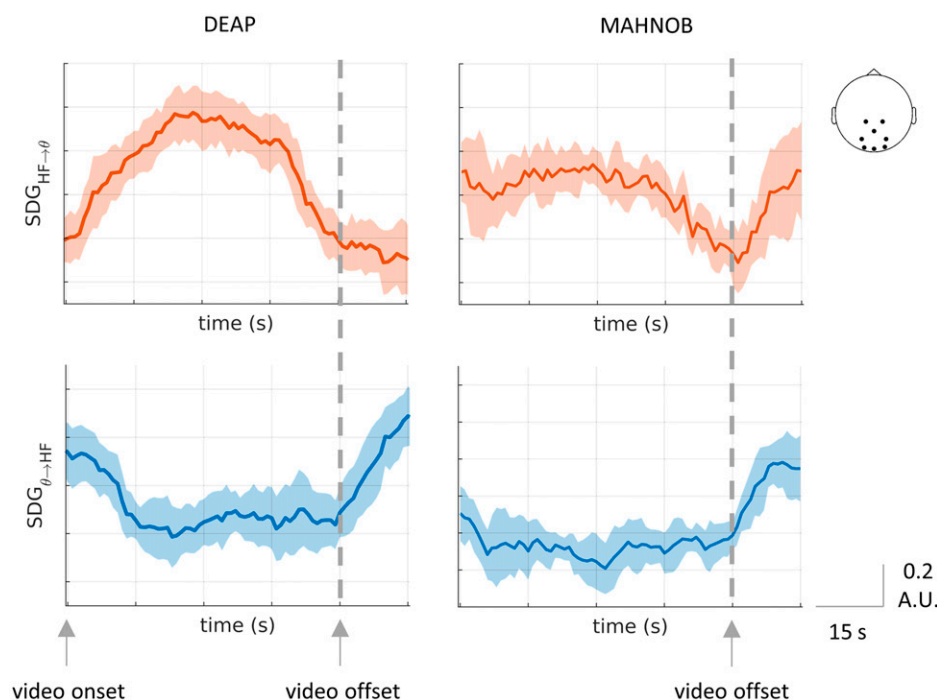

Fig. 6. Overall changes in the BHI during emotion elicitation in the HF-to-theta and theta-to-HF coefficients. Group-median ± MAD time course among subjects. All trials were averaged per each subject before computing the group medians. The trials were combined with respect to the video offset.
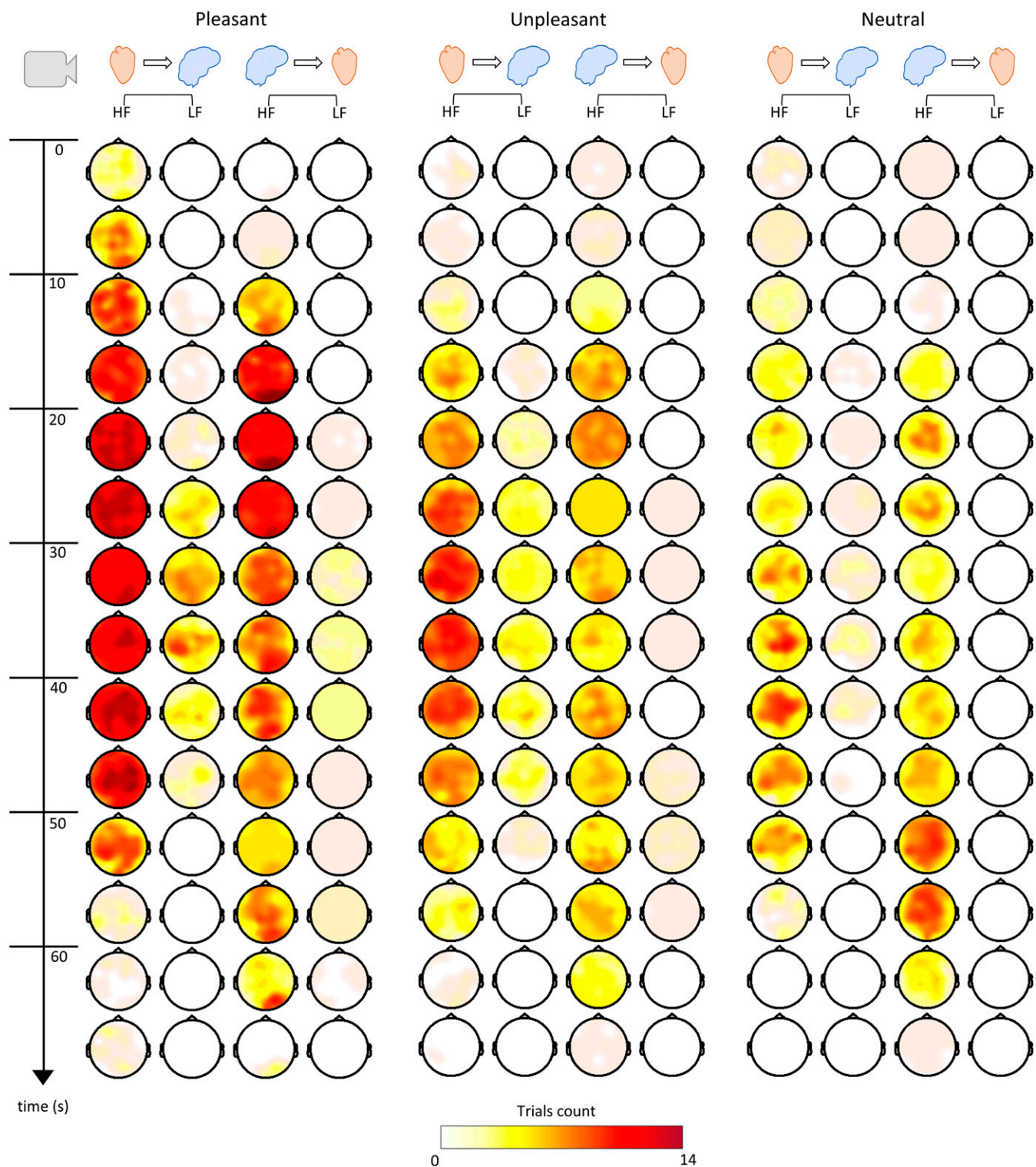
Fig. 7. BHI time course trial visualization. The scalp topographies displayed correspond to HF-to-brain, LF-to-brain, brain-to-HF, and brain-to-LF. Colormaps indicate the number of videos in which the 5-s group-median SDG coefficients during the emotion elicitation have been found significant compared to the rest coupling coefficients previously subtracted per subject.

activations in the frontal and parietal electrodes are observed in the HF-to-brain interplay, finishing with a guitar solo in which a brain-to-HF interplay is observed as well.

Results in *SI Appendix*, Fig. S16 are replicated in *SI Appendix*, Fig. S9 by considering different length of resting state.

At the end of this section, we remark that ascending BHI coupling (heart-to-brain) is the first in coming with respect to the descending (brain-to-heart) functional information exchange.

Discussion and Conclusion

This study aimed to tackle the question, What is the role of cardiac ANS activity in emotional processing? The ANS activity, controlling heartbeats and other visceral activities, has been widely associated with emotional processing (44) leading to a century-long debate on the role of the ANS in feelings (4). Recent studies have uncovered that ascending inputs from the

heart are involved in essential aspects of cognition, such as subjective perception, self-awareness, and consciousness (15, 45, 46). We used a mathematical modeling approach (32) to quantify the directional interplay between the physiological components gathered from the brain and the heart during emotion elicitation. The results show that cardiac parasympathetic activity plays a causal role in the processing of emotional arousal, sustaining both ascending and descending brain–heart interactions. To the best of our knowledge, major novelties of the current study with respect to prior state of the art are related to 1) the uncovering of the directed functional interplay between central and peripheral neural dynamics during an emotional elicitation, using ad-hoc mathematical models for synchronized EEG and ECG time series; 2) the uncovering of temporal dynamics of cortical and cardiovascular neural control during emotional processing in both ascending, from the heart to the brain, and descending, from the brain to the heart, functional directions; and 3) the experimental support for causation theories of physiological feelings.

In the frame of investigating the visceral origin of emotions, main findings of this study suggest that ascending BHI coupling initiates emotional processing and is mainly modulated by the subjective experience of emotional arousal. Such a relationship between arousal and ascending BHI may not be related to the attention levels, as controlled with two different neural correlates of attention. The main interactions begin through afferent vagal pathways (HF power) sustaining EEG oscillations, in which the theta band was repeatedly found related to major vagal modulations. In turn, with a later onset, this ascending modulation actually triggers a cascade of cortical neural activations that, in turn, modulate directed neural control onto the heart, namely from-brain-to-heart interplay. Concurrent bidirectional communication between the brain and body occurs throughout the emotional processing at specific timings, reaching a maximum coupling around 15 to 20 s from the elicitation onset, involving both cardiac sympathetic and vagal activity. Note that the simulation study reported in *Materials and Methods* demonstrates that nonspecific/causal changes in the variability of a single physiological signal do not modify per se the SDG-based estimation of functional BHI coupling, which is modulated by concurrent dynamical, nonrandom changes in both EEG and heartbeat series.

The observed ascending pathway of vagal activity toward cortical brain signals uniquely suggests that emotion processing is an integration of physiological inputs in the brain rather than an interpretation of physiological changes. The variation of the parasympathetic tone has been described before to be related to processes of fluctuations in attention and emotional processing (47). These autonomic markers have shown their capacity to correlate with emotions as subjectively described in healthy subjects (44) as well as under pathological conditions (48). The autonomic outflow has been previously correlated to behavior in polyvagal theory (49), describing neural circuits involved in homeostatic regulation and adaptation. Polyvagal theory describes the interaction of sympathetic and parasympathetic nervous systems, in which the parasympathetic branch is associated with emotion regulation because of its behavioral correlates with reactivity, the expression of emotion, and self-regulation skills (49). The mediating role of the vagus nerve during emotional processing fits with the communication loops observed in the BHI in our results. However, beyond mediation, we observed that parasympathetic activity initiates emotional processing. The observed ascending pathway of vagal activity toward the brain corroborates previous findings that heartbeats shape brain dynamics (12, 50). Therefore, this could

imply emotions are not the result of an interpretation of peripheral physiological changes but rather an integration of these inputs in the brain, from the visual, auditory, and somatosensory perception stages. Subjective emotional experiences might emerge from the ongoing evolution of this integration process.

The causal nature of ANS activity in feelings is consistent with physiological modeling and experimental data, as neurovisceral integration models indicate that neural circuits integrate central and autonomic responses related to emotions, with dynamic contextual adaptations (16, 21, 51). In theoretical developments, the specific role of bodily signals in subjectivity and consciousness has been conceived in different ways from the causation viewpoint. The somatic marker hypothesis of Damasio (5) affirms that the metarepresentation of bodily states constitutes an emotional feeling, generating a gut feeling, which influences cognitive processes. For some authors, visceral activity might provide information for the foundation of emotions (13, 18). For others, visceral activity is considered a central factor, where the neural monitoring of ascending visceral inputs is inherent for subjective perception, emotions, and consciousness (15, 52).

We showed that vagal modulations to the EEG theta oscillations primarily occurred during emotion elicitation, and these modulations were correlated with the perceived (reported) arousal but not with valence. These results are in line with an increasing amount of literature failing to highlight differences between neural concomitants of positive and negative valence. In contrast with the classical theories of emotions, studies on autonomic (53) and central nervous system (54, 55) dynamics failed to disentangle negative and positive valence, while specific differences in arousal were found independently of valence. Such results can be explained within the context of the valence general affective workspace hypothesis (56). Accordingly, valence is neither mapped in the brain across a monotonic dimension (from positive to negative) nor in valence-specific areas (54). On the contrary, several brain areas related to emotional regulation and expression seem to belong to a general workspace. In such a workspace, the neurons' firing indicates the presence of valence while the context in which they fire establishes the positive or negative valence.

The groupwise arousal was related to delta and theta bands in the frontal and occipitoparietal scalp regions as well as to the gamma band in temporal areas. To verify whether the results were related exclusively to the BHI, we performed the same analysis separately for brain and heart components, confirming that arousal changes cannot be explained by changes in cardiac parameters or EEG power by themselves. Moreover, the investigation of EEG correlates of attention through different biomarkers demonstrated that BHI coupling coefficients may not be related to attentional processes of the emotional elicitation.

The interactions between EEG activity and heart rate have been described previously in machine-learning studies, showing that the combination of these features in classifiers provides additional information related to consciousness and emotions (46, 57). Consistent with previous studies, BHI can describe certain cognitive states which cannot be explained by changes in cardiac parameters by themselves (22, 29, 58, 59). In particular, the relationship between heartbeat dynamics and theta band was previously described in the resting state, showing that heartbeats may induce theta synchronizations in defined brain networks (60). In this study, we showed that the theta band is actively modulated by vagal inputs under emotion elicitation (61). These results support the hypothesis that the peripheral inputs contribute to a first-person point of view for conscious/

subjective experiences (15). However, the relationship between the objective evaluation of psychophysiological parameters and the subjective experience has always to be taken with extreme caution. Furthermore, the functional BHI do not explain entirely the variance of arousal scores but the gap between subjective experience and the description of objective physiological changes remains to be bridged.

Theta activation has been repeatedly reported in different paradigms, such as the visualization of emotional faces (62) and emotional content in films (63). Our results corroborate a previous report (64) in which the midline frontal theta is associated with states of high arousal and high valence, followed by synchronization with posterior scalp areas. Previous studies have described that changes in theta are related to the level of arousal perceived (63, 65), although our results did not show a relationship in the theta band per se but rather in its afferent modulation from HF oscillations. The other EEG bands related to arousal were delta and gamma; however, few studies have reported such relations. The delta band has shown a potential involvement in emotional processing (66), and the close relationship between the theta and delta bands during emotional processing has been previously described as well (67). With respect to the gamma band, we believe that the arousal relation with the ascending modulations in temporal lobes could be somehow related to previous evidence linking theta and gamma bands, as an arousal-dependent synchronization (62).

Descending modulations were suppressed during the emotion elicitation tasks, particularly in the HF oscillations. The observed modulation involved a wide part of the EEG spectrum, from the alpha to the gamma band, with the alpha range being the most influential. The variations in brain-to-heart coefficients were stronger in the central scalp regions, with a slight extension toward the parietal and temporal areas, in contrast to the relation of alpha oscillations in emotions reported in other studies where it is related mainly to changes in frontal and prefrontal lobe activity (68). Less evidence is reported about beta and gamma oscillations in emotions; however, these higher frequencies are reported as a synchronized or desynchronized activity with respect to alpha (69) or theta bands (62). We could not distinguish the different types of emotions using information from the descending pathway, as we did not find associations with arousal or valence. However, we found that descending modulations were decreased in most of the trials compared to the resting state. Furthermore, descending changes were more delayed compared to the ascending pathway. This order of events strengthens the idea of a visceral origin of emotions. Studies on the somatosensory experience of feelings state that bodily sensations are felt in different body parts as a function of the type of emotions felt (70). In fact, the experience of others' emotions may be closely related to the activity in somatosensory cortex as well (71). The specific role of the descending pathway remains to be further investigated to determine whether it relates to bodily reexperiencing or to aspects other than the emotion itself but rather more general aspects, such as perception, attention, or memory (72, 73).

Several studies focused on BHI, feelings, and emotions in different paradigms have been conducted. To date, available evidence on BHI, feelings, and emotions describes dynamic and nonlinear interactions (16, 27, 30, 31). Further evidence exists in studies on heartbeat-evoked potentials; nevertheless, there is a lack of convergence in these results (29). For instance, some studies have tried to describe emotions by analyzing heartbeat-evoked potentials, for instance to explain valence (74, 75). In another study, heartbeat-evoked potentials were correlated with alpha power during the task with audiovisual stimuli

(76). However, as mentioned above, our results show that the SDG model in ascending modulations relates to the specific perceived arousal, and alpha activity is more related to the descending pathway. It remains unclear whether BHI measured from heartbeat-evoked potentials in healthy participants actually explains a part of valence, arousal, or other subjective aspects involved in emotion, such as ownership, motivation, dominance, or abnormalities in emotional processing. The most recent evidence in pathological conditions suggests a relationship between disrupted emotion recognition and heartbeat-evoked potentials, indicating that altered interoceptive mechanisms may interfere in priming emotions (50).

Affect (including valence and arousal) is an important component of emotion: Since the Schachter and Singer experiment the role of arousal in the onset of emotions was considered central (77). In this sense, the fact that physical arousal is the starter of the emotional reaction finds some confirmation in our results. However, the distinction between arousal (and affect in general) and emotions is underappreciated (2). According to several theoretical positions including the recent theory of constructed emotions (3, 78), affect is a component of emotions but not specific to a given emotion. Typically affect is defined as the "basic sense of feeling, ranging from unpleasant to pleasant (valence), and from idle to activated (arousal)" (79). Emotions integrate affect in a more complex mental phenomenon including, memory, other cognitive functions, and behavioral responses. Therefore, our results can be related not only to the entire emotional processing of arousal but also to affect-related aspects of a subjective experience. This would also explain why we were not able to differentiate different emotional states through a BHI analysis. While this may represent a limitation in the attempt to describe emotions through objective parameters, it also poses a step forward in the attempt to disentangle affect from emotion. In this regard, it is also important to note that the present research highlights the physiological components involved in the processing of a subjective experience. The lack of specificity of the physiological feelings and functional BHI indirectly supports that emotions correspond to predictive schemas arising from the integration of external and internal information that could also involve past experiences (3).

We repeatedly found two well-defined scalp regions in the midline frontal and occipitoparietal electrodes in which ascending BHI coefficients were concisely related to affect. These results suggest the possibility of multiple brain nodes participating in the ongoing process. Neuroimaging studies have shown evidence of the DMN and the processing of self-relevant and affective decisions (23), with the main nodes in the medial prefrontal cortex and posterior cingulate cortex. The fact that BHI is related to the DMN, in aspects including autonomic regulation (21) and interoception in self-related cognition (22), suggests that it may also be involved in emotional processing. The DMN, which is usually associated with passive states (80), presents an activation/deactivation behavior that seems to be related to the switch between inward mental activity and outward goal-directed activity (81). How the switching activity occurs is yet to be completely understood, but increasing evidence supports that the monitoring of the peripheral neural activity by the DMN may turn the brain to a goal and externally oriented mode in specific circumstances (81). Cardiac outputs might contribute to such a switch since they indirectly modulate DMN activity through projections to serotonergic raphe nuclei and noradrenergic locus coeruleus (82). While interoception might be mapped elsewhere in the cortex (primary and secondary sensory cortex and insula, among others)

(14, 18), DMN might receive interoceptive information to promote its deactivation and desynchronization as a part of the process that leads to the goal-oriented response. In this regard, having DMN node activations as a function of the level of arousal may imply that the higher the arousal, the higher the system is directed from inward out. The idea that peripheral physiological reactions trigger the DMN switch and contribute to the start a of goal-oriented response is in line with classical theories stating that emotions are a complex reaction to respond to relevant external stimuli (83). It is also interesting to note that the CAN and DMN share a part of the brain structures, for example the medial prefrontal cortex. As a partially alternative framework of interpretation, it is interesting to note that the DMN has been also described as a network for integration and online updating of experiences (3, 84). Indeed, bridging the internal state with external relevant information is expected to occur during the emotional experience.

The interplay between the CNS and ANS involves not only the brain and heart but also other bodily signals, such as electrodermal activity, breathing, gastrointestinal activity, or pupil diameter (85). We believe that the proposed analysis can be enriched in future work at a multisystem level. Furthermore, even though we employed two large and publicly available datasets (33, 34), one may argue about how our results are bound to the specific emotional elicitation (video presentation) and how BHI might vary according to different emotional elicitation techniques, which represent an interesting further line of investigation. Note that resting state periods were used as a control for some of our emotional processing study. In the MAHNOB dataset, data analysis on neutral videos was not performed because of their short duration (up to 20 s), and the dataset does not provide continuous recordings for different videos. This constitutes a study limitation as neutral videos may allow for a better disentangling of emotion properties (valence, arousal) as compared with the many differences that exist between rest periods and videos. Moreover, results on DEAP and MAHNOB datasets show some differences especially related to the magnitude and distribution over the scalp of the statistical indices. Some important factors that may lead to such differences include that the DEAP dataset is stored as a continuous recording throughout sessions, whereas MAHNOB recordings are separated per trial and were preprocessed independently; the DEAP dataset has shorter intervals between emotional trials of different length than MAHNOB, which implies fewer recovery periods for the neurophysiological responses. Note that our claim does not point to a specific scalp distribution of the BHI coupling indices, but our main finding indicates that subjective emotional arousal modulates ascending functional BHI coupling. Concerning the timing, while the SDG model cannot assess spontaneous neural responses in a millisecond resolution, as heartbeat-evoked potentials do, it has the advantage of assessing ongoing, continuous, and bidirectional modulations.

The tight relationship between well-being and autonomic function is evidenced in cases of dysfunctional BHI in psychopathological conditions (86). Promising developments may lead to a better understanding of emotional processing and bodily states, as clinical applications involving the analysis of brain–heart interactions have brought overall important advances (46, 87, 88). Beyond mental and neurological health, a vast amount of evidence shows that other bodily activities actively react as a function of ongoing brain activity, including gut activity, endocrine responses, and inflammation (14), indicating the importance of neural homeostasis in the human body. Our results may be expanded to better clarify the role of the BHI in the mutual vulnerability between mental and physical conditions and thus provide a psychophysiological model of how physical health may contribute to mental health risk factors, and vice versa.

The use of secondary, previously released, data raises the issue of challenges and problems with the preregistration process and the other standard polices to ensure good research practices. While, in a strict sense, preregistration has been developed and widely used for primary data, the use of secondary data poses several difficulties with standard preregistration as recently discussed (89, 90). While a general agreement on the most correct approach is still lacking, a relevant suggestion is to declare the working hypothesis in advance (90). Such statements have been done in previous scientific peer-reviewed publications from the authors, in which it is stated that ascending afferents to the brain play a role in shaping perception, consciousness, and emotions (43, 46, 52, 61, 91). Moreover, the use of public data and the availability of our analysis pipeline comes with the advantage that our results can go through a complete replication analysis. Finally, the available pipeline could be used for future replication studies undergoing preregistration or published as registered report (90).

In conclusion, we have shown experimentally how the dynamic interplay between the central and autonomic peripheral nervous systems sustains emotional experiences through specific timings and cortical areas. During emotional elicitation, we have shown how autonomic dynamics on cardiovascular control initiate the physiological response to emotion in the direction of the CNS, possibly belonging to the DMN and CAN. This activity is correlated with arousal. Our results add new momentum to the theory of emotions, suggesting that peripheral neural dynamics of the cardiovascular ANS may trigger the emotional process at the brain level.

1. W. James, What is an emotion? *Mind* **9**, 188–205 (1884).
2. R. Adolphs, L. Mlodinow, L. F. Barrett, What is an emotion? *Curr. Biol.* **29**, R1060–R1064 (2019).
3. L. F. Barrett, The theory of constructed emotion: An active inference account of interoception and categorization. *Soc. Cogn. Affect. Neurosci.* **12**, 1–23 (2017).
4. E. F. Pace-Schott *et al.*, Physiological feelings. *Neurosci. Biobehav. Rev.* **103**, 267–304 (2019).
5. A. Damasio, *The Feeling of What Happens: Body and Emotion in the Making of Consciousness* (Harcourt College Publishers, 1999).
6. R. Brewer, R. Cook, G. Bird, Alexithymia: A general deficit of interoception. *R. Soc. Open Sci.* **3**, 150664 (2016).

7. C. G. Kooiman, P. Spinhoven, R. W. Trijsburg, The assessment of alexithymia: A critical review of the literature and a psychometric study of the Toronto Alexithymia Scale-20. *J. Psychosom. Res.* **53**, 1083–1090 (2002).
8. W. G. Chen *et al.*, The emerging science of interoception: Sensing, integrating, interpreting, and regulating signals within the self. *Trends Neurosci.* **44**, 3–16 (2021).
9. A. Fujimoto, E. A. Murray, P. H. Rudebeck, Interaction between decision-making and interoceptive representations of bodily arousal in frontal cortex. *Proc. Natl. Acad. Sci. U.S.A.* **118**, e2014781118 (2021).
10. D. Azzalini, A. Buot, S. Palminteri, C. Tallon-Baudry, Responses to heartbeats in ventromedial prefrontal cortex contribute to subjective preference-based decisions. *J. Neurosci.* **41**, 5102–5114 (2021).

11. A. R. Damasio *et al.*, Subcortical and cortical brain activity during the feeling of self-generated emotions. *Nat. Neurosci.* **3**, 1049–1056 (2000).

12. H.-D. Park, S. Correia, A. Ducorps, C. Tallon-Baudry, Spontaneous fluctuations in neural responses to heartbeats predict visual detection. *Nat. Neurosci.* **17**, 612–618 (2014).

13. A. D. Craig, How do you feel–now? The anterior insula and human awareness. *Nat. Rev. Neurosci.* **10**, 59–70 (2009).

14. H. D. Critchley, S. N. Garfinkel, Interoception and emotion. *Curr. Opin. Psychol.* **17**, 7–14 (2017).

15. D. Azzalini, I. Rebollo, C. Tallon-Baudry, Visceral signals shape brain dynamics and cognition. *Trends Cogn. Sci.* **23**, 488–509 (2019).

16. J. F. Thayer, R. D. Lane, A model of neurovisceral integration in emotion regulation and dysregulation. *J. Affect. Disord.* **61**, 201–216 (2000).

17. O. G. Cameron, Interoception: The inside story–A model for psychosomatic processes. *Psychosom. Med.* **63**, 697–710 (2001).

18. A. D. Craig, How do you feel? Interoception: The sense of the physiological condition of the body. *Nat. Rev. Neurosci.* **3**, 655–666 (2002).

19. F. Beissner, K. Meissner, K.-J. Bär, V. Napadow, The autonomic brain: An activation likelihood estimation meta-analysis for central processing of autonomic function. *J. Neurosci.* **33**, 10503–10511 (2013).

20. G. Valenza *et al.*, The central autonomic network at rest: Uncovering functional MRI correlates of time-varying autonomic outflow. *Neuroimage* **197**, 383–390 (2019).

21. J. F. Thayer, F. Ahs, M. Fredrikson, J. J. Sollers III, T. D. Wager, A meta-analysis of heart rate variability and neuroimaging studies: Implications for heart rate variability as a marker of stress and health. *Neurosci. Biobehav. Rev.* **36**, 747–756 (2012).

22. M. Babo-Rebelo, C. G. Richter, C. Tallon-Baudry, Neural responses to heartbeats in the default network encode the self in spontaneous thoughts. *J. Neurosci.* **36**, 7829–7840 (2016).

23. J. R. Andrews-Hanna, J. S. Reidler, J. Sepulcre, R. Poulin, R. L. Buckner, Functional-anatomic fractionation of the brain's default network. *Neuron* **65**, 550–562 (2010).

24. H. D. Critchley, D. R. Corfield, M. P. Chandler, C. J. Mathias, R. J. Dolan, Cerebral correlates of autonomic cardiovascular arousal: A functional neuroimaging investigation in humans. *J. Physiol.* **523**, 259–270 (2000).

25. K. L. Phan, T. Wager, S. F. Taylor, I. Liberzon, Functional neuroanatomy of emotion: A meta-analysis of emotion activation studies in PET and fMRI. *Neuroimage* **16**, 331–348 (2002).

26. S. Anders *et al.*, Parietal somatosensory association cortex mediates affective blindsight. *Nat. Neurosci.* **7**, 339–340 (2004).

27. M. D. Lewis, Bridging emotion theory and neurobiology through dynamic systems modeling. *Behav. Brain Sci.* **28**, 169–194, discussion 194–245 (2005).

28. D. Candia-Rivera, V. Catrambone, G. Valenza, The role of electroencephalography electrical reference in the assessment of functional brain-heart interplay: From methodology to user guidelines. *J. Neurosci. Methods* **360**, 109269 (2021).

29. H.-D. Park, O. Blanke, Heartbeat-evoked cortical responses: Underlying mechanisms, functional roles, and methodological considerations. *Neuroimage* **197**, 502–511 (2019).

30. V. Catrambone, A. Greco, E. P. Scilingo, G. Valenza, Functional linear and nonlinear brain–heart interplay during emotional video elicitation: A maximum information coefficient study. *Entropy (Basel)* **21**, 892 (2019).

31. A. Greco *et al.*, Lateralization of directional brain-heart information transfer during visual emotional elicitation. *Am. J. Physiol. Regul. Integr. Comp. Physiol.* **317**, R25–R38 (2019).

32. V. Catrambone, A. Greco, N. Vanello, E. P. Scilingo, G. Valenza, Time-resolved directional brain-heart interplay measurement through synthetic data generation models. *Ann. Biomed. Eng.* **47**, 1479–1489 (2019).

33. S. Koelstra *et al.*, DEAP: A database for emotion analysis; Using physiological signals. *IEEE Trans. Affect. Comput.* **3**, 18–31 (2012).

34. M. Soleymani, J. Lichtenauer, T. Pun, M. Pantic, A multimodal database for affect recognition and implicit tagging. *IEEE Trans. Affect. Comput.* **3**, 42–55 (2012).

35. R. Oostenveld, P. Fries, E. Maris, J.-M. Schoffelen, FieldTrip: Open source software for advanced analysis of MEG, EEG, and invasive electrophysiological data. *Comput. Intell. Neurosci.* **2011**, 156869 (2011).

36. L. J. Gabard-Durnam, A. S. Mendez Leal, C. L. Wilkinson, A. R. Levin, The Harvard automated processing pipeline for electroencephalography (HAPPE): Standardized processing software for developmental and high-artifact data. *Front. Neurosci.* **12**, 97 (2018).

37. L. Citi, E. N. Brown, R. Barbieri, A real-time automated point-process method for the detection and correction of erroneous and ectopic heartbeats. *IEEE Trans. Biomed. Eng.* **59**, 2828–2837 (2012).

38. M. Orini, R. Bailón, L. T. Mainardi, P. Laguna, P. Flandrin, Characterization of dynamic interactions between cardiovascular signals by time-frequency coherence. *IEEE Trans. Biomed. Eng.* **59**, 663–673 (2012).

39. M. Brennan, M. Palaniswami, P. Kamen, Poincaré plot interpretation using a physiological model of HRV based on a network of oscillators. *Am. J. Physiol. Heart Circ. Physiol.* **283**, H1873–H1886 (2002).

40. H. Al-Nashash, Y. Al-Assaf, J. Paul, N. Thakor, EEG signal modeling using adaptive Markov process amplitude. *IEEE Trans. Biomed. Eng.* **51**, 744–751 (2004).

41. S. Whitmarsh, C. Gitton, V. Jousmäki, J. Sackur, C. Tallon-Baudry, Neuronal correlates of the subjective experience of attention. *Eur. J. Neurosci.*, 10.1111/ejn.15395 (2021).

42. M. Vázquez Marrufo, E. Vaquero, M. J. Cardoso, C. M. Gómez, Temporal evolution of α and β bands during visual spatial attention. *Brain Res. Cogn. Brain Res.* **12**, 315–320 (2001).

43. D. Candia-Rivera, V. Catrambone, R. Barbieri, G. Valenza, Functional assessment of bidirectional cortical and peripheral neural control on heartbeat dynamics: A brain-heart study on thermal stress. *Neuroimage* **251**, 119023 (2022).

44. S. D. Kreibig, Autonomic nervous system activity in emotion: A review. *Biol. Psychol.* **84**, 394–421 (2010).

45. A. S. Klein, N. Dolensek, C. Weiand, N. Gogolla, Fear balance is maintained by bodily feedback to the insular cortex in mice. *Science* **374**, 1010–1015 (2021).

46. D. Candia-Rivera *et al.*, Neural responses to heartbeats detect residual signs of consciousness during resting state in postcomatose patients. *J. Neurosci.* **41**, 5251–5262 (2021).

47. J. F. Thayer, G. J. Siegle, Neurovisceral integration in cardiac and emotional regulation. *IEEE Eng. Med. Biol. Mag.* **21**, 24–29 (2002).

48. L. Vazquez *et al.*, High frequency heart-rate variability predicts adolescent depressive symptoms, particularly anhedonia, across one year. *J. Affect. Disord.* **196**, 243–247 (2016).

49. S. W. Porges, The polyvagal perspective. *Biol. Psychol.* **74**, 116–143 (2007).

50. P. C. Salamone *et al.*, Interoception primes emotional processing: Multimodal evidence from neurodegeneration. *J. Neurosci.* **41**, 4276–4292 (2021).

51. D. Hagemann, S. R. Waldstein, J. F. Thayer, Central and autonomic nervous system integration in emotion. *Brain Cogn.* **52**, 79–87 (2003).

52. R. Smith, J. F. Thayer, S. S. Khalsa, R. D. Lane, The hierarchical basis of neurovisceral integration. *Neurosci. Biobehav. Rev.* **75**, 274–296 (2017).

53. J. F. Brosschot, J. F. Thayer, Heart rate response is longer after negative emotions than after positive emotions. *Int. J. Psychophysiol.* **50**, 181–187 (2003).

54. K. A. Lindquist, A. B. Satpute, T. D. Wager, J. Weber, L. F. Barrett, The brain basis of positive and negative affect: Evidence from a meta-analysis of the human neuroimaging literature. *Cereb. Cortex* **26**, 1910–1922 (2016).

55. J. Min *et al.*, Emotion down-regulation targets interoceptive brain regions while emotion up-regulation targets other affective brain regions. *J. Neurosci.* **42**, 2973–2985 (2022).

56. L. F. Barrett, E. Bliss-Moreau, Affect as a psychological primitive. *Adv. Exp. Soc. Psychol.* **41**, 167–218 (2009).

57. J. Marín-Morales *et al.*, Affective computing in virtual reality: Emotion recognition from brain and heartbeat dynamics using wearable sensors. *Sci. Rep.* **8**, 13657 (2018).

58. M. Naji, G. P. Krishnan, E. A. McDevitt, M. Bazhenov, S. C. Mednick, Coupling of autonomic and central events during sleep benefits declarative memory consolidation. *Neurobiol. Learn. Mem.* **157**, 139–150 (2019).

59. P.-C. Chen, L. N. Whitehurst, M. Naji, S. C. Mednick, Autonomic/central coupling benefits working memory in healthy young adults. *Neurobiol. Learn. Mem.* **173**, 107267 (2020).

60. J. Kim, B. Jeong, Heartbeat induces a cortical theta-synchronized network in the resting state. *eNeuro* **6**, ENEURO.0200-19.2019 (2019).

61. E. Patron, R. Mennella, S. Messerotti Benvenuti, J. F. Thayer, The frontal cortex is a heart-brake: Reduction in delta oscillations is associated with heart rate deceleration. *Neuroimage* **188**, 403–410 (2019).

62. M. Balconi, U. Pozzoli, Arousal effect on emotional face comprehension: Frequency band changes in different time intervals. *Physiol. Behav.* **97**, 455–462 (2009).

63. C. M. Krause, V. Viemerö, A. Rosenqvist, L. Sillanmäki, T. Aström, Relative electroencephalographic desynchronization and synchronization in humans to emotional film content: An analysis of the 4-6, 6-8, 8-10 and 10-12 Hz frequency bands. *Neurosci. Lett.* **286**, 9–12 (2000).

64. L. I. Aftanas, S. A. Golocheikine, Human anterior and frontal midline theta and lower alpha reflect emotionally positive state and internalized attention: High-resolution EEG investigation of meditation. *Neurosci. Lett.* **310**, 57–60 (2001).

65. L. I. Aftanas, A. A. Varlamov, S. V. Pavlov, V. P. Makhnev, N. V. Reva, Time-dependent cortical asymmetries induced by emotional arousal: EEG analysis of event-related synchronization and desynchronization in individually defined frequency bands. *Int. J. Psychophysiol.* **44**, 67–82 (2002).

66. M. A. Klados *et al.*, A framework combining delta event-related oscillations (EROs) and synchronisation effects (ERD/ERS) to study emotional processing. *Comput. Intell. Neurosci.* **2009**, 549419 (2009).

67. G. G. Knyazev, J. Y. Slobodskoj-Plusnin, A. V. Bocharov, Event-related delta and theta synchronization during explicit and implicit emotion processing. *Neuroscience* **164**, 1588–1600 (2009).

68. J. J. B. Allen, J. A. Coan, M. Nazarian, Issues and assumptions on the road from raw signals to metrics of frontal EEG asymmetry in emotion. *Biol. Psychol.* **67**, 183–218 (2004).

69. S. Jessen, S. A. Kotz, The temporal dynamics of processing emotions from vocal, facial, and bodily expressions. *Neuroimage* **58**, 665–674 (2011).

70. L. Nummenmaa, R. Hari, J. K. Hietanen, E. Glerean, Maps of subjective feelings. *Proc. Natl. Acad. Sci. U.S.A.* **115**, 9198–9203 (2018).

71. A. Sel, B. Calvo-Merino, M. Tsakiris, B. Forster, The somatotopy of observed emotions. *Cortex* **129**, 11–22 (2020).

72. L. Pessoa, On the relationship between emotion and cognition. *Nat. Rev. Neurosci.* **9**, 148–158 (2008).

73. V. R. LeBlanc, M. M. McConnell, S. D. Monteiro, Predictable chaos: A review of the effects of emotions on attention, memory and decision making. *Adv. Health Sci. Educ. Theory Pract.* **20**, 265–282 (2015).

74. B. Couto *et al.*, Heart evoked potential triggers brain responses to natural affective scenes: A preliminary study. *Auton. Neurosci.* **193**, 132–137 (2015).

75. J. Kim *et al.*, Sad faces increase the heartbeat-associated interoceptive information flow within the salience network: A MEG study. *Sci. Rep.* **9**, 430 (2019).

76. C. D. B. Luft, J. Bhattacharya, Aroused with heart: Modulation of heartbeat evoked potential by arousal induction and its oscillatory correlates. *Sci. Rep.* **5**, 15717 (2015).

77. S. Schachter, J. E. Singer, Cognitive, social, and physiological determinants of emotional state. *Psychol. Rev.* **69**, 379–399 (1962).

78. L. F. Barrett, Emotions are real. *Emotion* **12**, 413–429 (2012).

79. L. F. Barrett, *How Emotions Are Made* (Pan Macmillan, 2017).

80. M. E. Raichle, The brain's default mode network. *Annu. Rev. Neurosci.* **38**, 433–447 (2015).

81. F. Riemer *et al.*, Dynamic switching between intrinsic and extrinsic mode networks as demands change from passive to active processing. *Sci. Rep.* **10**, 21463 (2020).

82. S. Tumati, M. P. Paulus, G. Northoff, Out-of-step: Brain-heart desynchronization in anxiety disorders. *Mol. Psychiatry* **26**, 1726–1737 (2021).

83. A. S. Fox, R. C. Lapate, A. J. Shackman, R. J. Davidson, Eds., *The Nature of Emotion: Fundamental Questions* (Oxford University Press, ed. 2, 2018).

84. Y. Yeshurun, M. Nguyen, U. Hasson, The default mode network: Where the idiosyncratic self meets the shared social world. *Nat. Rev. Neurosci.* **22**, 181–192 (2021).

85. I. Rebollo, A.-D. Devauchelle, B. Béranger, C. Tallon-Baudry, Stomach-brain synchrony reveals a novel, delayed-connectivity resting-state network in humans. *eLife* **7**, e33321 (2018).

86. T. P. Beauchaine, J. F. Thayer, Heart rate variability as a transdiagnostic biomarker of psychopathology. *Int. J. Psychophysiol.* **98**, 338–350 (2015).

87. J. Terhaar, F. C. Viola, K.-J. Bär, S. Debener, Heartbeat evoked potentials mirror altered body perception in depressed patients. *Clin. Neurophysiol.* **123**, 1950–1957 (2012).

88. L. Perogamvros *et al.*, Increased heartbeat-evoked potential during REM sleep in nightmare disorder. *Neuroimage Clin.* **22**, 101701 (2019).

89. O. van den Akker *et al.*, Preregistration of secondary data analysis: A template and tutorial. *PsyArXiv* [Preprint] (2019). https://doi.org/10.31234/osf.io/hvfmr (Accessed 28 February 2022).

90. J. R. Baldwin, J.-B. Pingault, T. Schoeler, H. M. Sallis, M. R. Munafò, Protecting against researcher bias in secondary data analysis: Challenges and potential solutions. *Eur. J. Epidemiol.* **37**, 1–10 (2022).

91. M. Mather, J. Thayer, How heart rate variability affects emotion regulation brain networks. *Curr. Opin. Behav. Sci.* **19**, 98–104 (2018).